Optical Materials 149 (2024) 115056

Contents lists available at ScienceDirect

Optical Materials

journal homepage: www.elsevier.com/locate/optmat

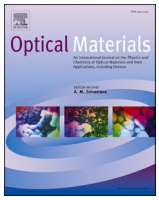

Research Article

Environmental influences of BaO on structure and ligand field parameters of Co^{2+} inside $K_2O–AL_2O_3–CoO–BaO–B_2O_3$ glass

Hesham Y. Amin [a,h,i,*], A. Samir [b,****], Moukhtar A. Hassan [c,**], F. Ahmad [d], Aly Saeed [e], M. S. Sadeq [f,g,***]

[a] Research & Studies Center, Midocean University, Moroni, 6063, Comoros
[b] Basic Science Department, Faculty of Engineering at Shoubra, Benha University, 11629, Cairo, Egypt
[c] Physics Department, Faculty of Science, Al-Azhar University, 11884, Cairo, Egypt
[d] Physics Department, Faculty of Science, Al-Azhar University (Girls Branch), 11754, Cairo, Egypt
[e] Mathematical and Natural Science Department, Faculty of Engineering, Egyptian Russian University, Badr City, Cairo, Egypt
[f] Department of Basic Science, Faculty of Engineering, Sinai University – Kantara Branch, 41636, Ismailia, Egypt
[g] MEU Research Unit, Middle East University, Amman, Jordan
[h] School of Information and Electrical Engineering, Hangzhou City University, No. 48, Huzhou Street, Hangzhou, 310015, China
[i] State Key Laboratory of Modern Optical Instrumentation, College of Optical Science and Engineering, Zhejiang University, Hangzhou, 310027, China

ARTICLE INFO

Keywords:
CoO
BaO
Optical transitions
Alumino-borate glass
Ligand field parameters

ABSTRACT

The study of transition metal cations containing glass is a very important topic due to the need for new colored glass used in several optical applications. One of these transition metal cations is cobalt (Co) which have more than valence state (Co^{3+} and Co^{2+}). Here, alumino-borate glass doped with constant cobalt oxide (CoO) content and different contents of barium oxide (BaO) were prepared by the melt-quenching technique. Structurally, the samples density increases, and the molar volume decreases with further additions of BaO. Also, FTIR spectra confirmed the presence of AlO_4, AlO_6, BO_3, and BO_4 structural units. Optically, it is confirmed that the absorption bands at about 574 nm and 1413 nm which are associated with $^4A_2(^4F) \rightarrow ^4T_1(^4P)$ and with $^4A_2(^4F) \rightarrow ^4T_1(^4F)$ optical transitions, respectively of Co^{2+} cations in tetrahedral coordination. These two optical transitions were used to study the ligand field parameters ($10Dq$ and B). Also, these parameters were used to explain the environmental influences of BaO on the bonding nature between Co cations and their ligands. With increasing BaO content, the d-orbital shrinkage and high interaction between d-electrons of Co^{2+} ions result in a high tendency toward the ionicity of the bond nature between Co^{2+} ions and their ligands. Finally, we concluded the significant influence of BaO addition on the structure, electronic transitions and ligand field parameters of cobalt alumino-borate glasses.

1. Introduction

Among all glass families, borate glass is one of the most prevalent glass network formers. Due to its distinct properties and applications, it has drawn a lot of attention from researchers [1,2]. It is well-known that boron atom can exist in glasses in form tetrahedral coordination (BO_4) and trigonal coordinated units (BO_3). The content and transformation between these coordination control the properties of borate glass materials. In addition to borate glass has an excellent UV and visible transparency, required thermal stability, moderate chemical durability, and low melting point [3]. Therefore, owing to their appealing properties, borate glasses are highly desirable candidates for several high-tech applications such as optical devices, thermal sensors, biomaterials, laboratories equipment's, lasers, and optical fibers [4,5].

Bewitchingly, glasses including transition metal ions were found to have distinctive colors and, as a result, they acquire distinctive optical

* Corresponding author. Research & Studies Center, Midocean University, Moroni, 6063, Comoros.
** Corresponding author.
*** Corresponding author. Basic Science Department, Faculty of Engineering, Sinai University, Egypt.
**** Corresponding author.
E-mail addresses: hesham_yahia25@yahoo.com (H.Y. Amin), ahmed.soliman01@feng.bu.edu.eg (A. Samir), m.a.hassan@azhar.edu.eg (M.A. Hassan), mhmd_sa3d@hotmail.com (M.S. Sadeq).

https://doi.org/10.1016/j.optmat.2024.115056
Received 21 September 2023; Received in revised form 17 January 2024; Accepted 6 February 2024

features. The transition metal cations, for many decades, have become known to the researchers due to their effectiveness for exploiting in optical sectors. It is well-recognized that transition metal cations have incomplete 3d shells. The optical active 3d electrons are existing in the outer shell of cations and interact with the electric fields of the surrounding anions, thus, they are used as spectroscopic probes to inspect the impacts of structural modifications on the structure-properties relationships. A wide range of applications were reported for transition metal ions doped glasses such as optical fiber devices for communication instruments, solid-states laser, and concentrators of luminescent solar panels, solid battery, optical filters, memories, and electronic equipment [6,7]. Among different transition metal oxides, cobalt oxide is one of such familiar oxides that are used effectively in glass doping. Divalent Cobalt cations (Co^{2+}) present in glasses in two coordination sites octahedral and/or tetrahedral [8]. In particular, Co^{2+} ions, with $3d^7$ configuration, have unfilled orbitals that allows to electrons to transfer, giving distinctive optical transitions in the visible region. These transitions impart the glass material their different color. Depending on the chemical composition, the color palette varies from blue to pink, passing with violet color. Also, the transition from tetrahedral to octahedral symmetry and vice-versa contributes these color span [9–11]. Ligand field theory is one of such theoretical methods that have concerned to study the color variations and the chemical environments surrounding the transition metal cations in glasses to explore the structural-properties relationships. Numerous researchers have thoroughly investigated the cobalt ions intercalated into glass material in terms of ligand field theory [5,12–15]. Our work is presented to focus on the impact of alkalinity modifications on ligand field and its relationship with other properties of cobalt ions in borate glass.

The additions of aluminum oxide (Al_2O_3) to glass material was observed to enhance mechanical features, improve optical responsibility, increase the density, induce a high refractive index, enhance chemical resistance, decrease the opacity, and support the glass stability of the composition [4,5,16,17]. Trivalent Aluminum ions have three coordination states in glass, four-fold coordination (with structural unit O_4), five-fold coordination (with structural unit O_5) and six-fold coordination (with structural unit O_6) structural units [18]. When it associates with boron oxide, a new glass network originates, namely, alumino-borate glass network. The alumino-borate glass network has combined the features of both borate and aluminate networks. The alumino-borate glass material has charming physical properties such as the high resistance to moisture, good chemical resistance, best optical features, decreased thermal expansion required for working devices, acceptable mechanical durability, and low toxicity [4,5,19]. Due to these appealing properties of alumino-borate glass, the researchers have exploited it in high-technological applications such as microwave cavities, dental cements, crucibles, and battery separators [4,5,17]. Recently, the physical features of alumino-borate glass such as structural, optical, luminescence, thermal, and electrical properties have studied by Morshidy et al. [4,5,19], Doweidar et al. [20], Mohan et al. [21], Dias et al. [22], Kaura et al. [23], Sadeq and Abdo [24].

In this regard, the alumino-borate glass network exhibits pivotal modifications of its physicochemical properties in terms of the alkali-alkaline content. The compositional evolution of [B_2O_3 - Al_2O_3 - CoO] glass system was made through the alkalinity modifications. Here, we study the alkalinity modifications by adding the barium oxide at the expense of potassium oxide with content variation (0–20 mol %). The influence of BaO on structural features including density, molar volume, interatomic distances, Co ions concentration, and infrared absorption spectra of glass network was described. As well as the influence of BaO on optical properties were presented including the electronic transitions of Co ions in tetrahedral sites at ~ 574 nm and ~ 1413 nm. Furthermore, the ligand field parameters such as ligand field splitting (10 Dq), Racah parameters (B and C), nephelauxetic ratio, covalency reduction factor, and Slater-Condon parameters (F_2 and F_4).

2. Experimental methodology

Cobalt-alumino-borate glass system with the following formula were successfully prepared employing the conventional melt quenching technique; [x BaO – (20-x) K_2O – 63.5 B_2O_3 – 15 Al_2O_3 – 1.5 CoO]. Barium oxide was loaded at the expense of potassium oxide with content from 0 mol % reaching 20 mol%. High purity raw materials including H_3BO_3 (Nasr Pharmaceutical, ≥ 98.5, Egypt), K_2CO_3 (Loba, ≥ 99, India), CoO (BDH chemicals Poole, ≥ 99.8, England), $BaCO_3$ (Loba, ≥ 99, India) and Al_2O_3 (Alfa Aesar, ≥ 99.8, USA), were utilized as starting ingredients. These substances are weighed in accordance with their mol % using an electronic balance with a 0.001 g accuracy, where each sample has batch weight of 25 g. Then, they ground in an agate mortar until a uniform mixture is achieved. Thereafter, the powder put into crucibles, which made from porcelain, in an electrical furnace to carbonize at 600 °C for 30 min then increasing the temperature at 1180 °C for 45 min. The melting process occurred at [1100°C–1180 °C], depending on chemical composition. The resulting molten was carefully stirred to ensure some homogeneity of glass specimens. Finally, the resulting molten was poured and quenched at room temperature between two smoothed copper plates. The obtained specimens at the end of preparation were bubble-free, as shown in Fig. 1.

To measure the density values of specimens, Archimedes' principle was exploited to do this task. Toluene, with a density of 0.866 $g.cm^{-3}$, was used as an immersion liquid. Moreover, the density measurements were carried out using the above-mentioned digital balance. The density measurement was repeated five times and obtaining the averaged and the experimenta error. The infrared data were collected using FT-IR Spectrometers type of (Nicolet iS50 - Thermo Fisher Scientific). The FTIR data were collected at room temperature (RT) in the absorbance mode in wavenumbers ranges of (400–4000 cm^{-1}). To measure the optical absorption measurements, the samples were polished finely to obtain glass samples with a thickness of about 0.7 mm. Optical absorbance spectra were measured using UV–VIS–NIR spectrophotometer in the wavelength range (200–2500 nm). The optical system of JASCO-V-670 spectrophotometer is a double beam single monochromator. The photometric mode is an absorbance with a medium response. The resolution is 1 nm. The spectral bandwidth of UV–Vis region is 2 nm and for NIR region is 40 nm. The wavelength repeatability of UV–Vis region is ±0.05 nm and for NIR region is ±0.2 nm. The data interval is 2 nm, with a scan speed of 1000 nm/min, a change source at 340 nm, a change grating at 850 nm, and a light source of D2/WI.

3. Results and discussion

3.1. Density and molar volume

Density is a characteristic physical property that is sensitive to the internal structural variations of glass material. In this regard, we used density technique to observe the impacts of compositions change on the structural variations. Here, Archimedean method was utilized to measure the density of all glass specimens. Fig. 2 (a) depicts the increase in the measured density with increasing barium contents. It is noticed that the experimental density was augmented from 2.120 g cm^{-3} reaching 2.802 g cm^{-3} (i.e., increased to 32 %), with an experimental error about

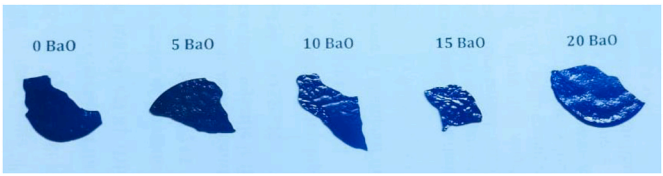

Fig. 1. Photograph of prepared glass samples.

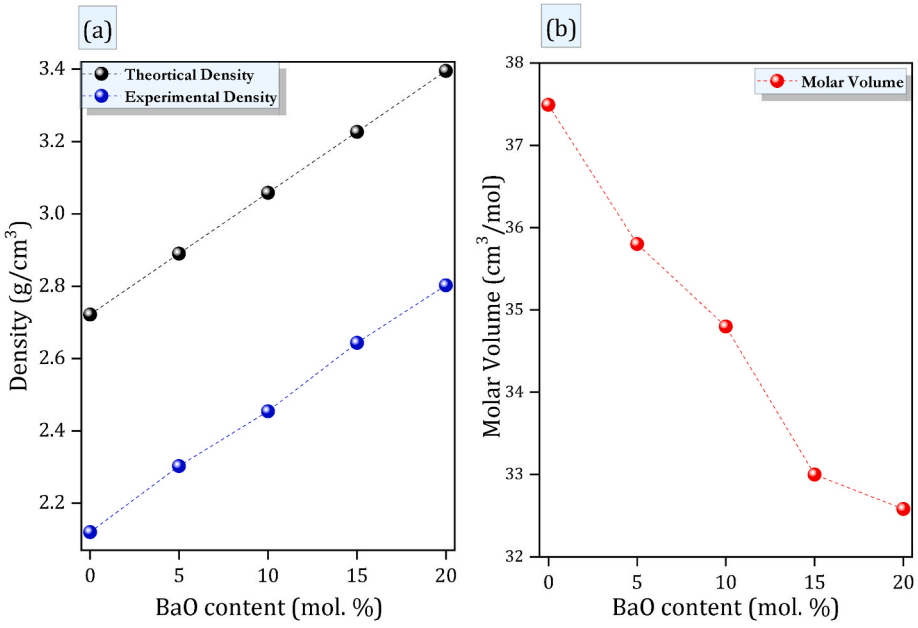

Fig. 2. (A) Comparison between the experimental and theoretical densities variations versus BaO contents and (B) Variations of molar volume versus BaO contents for **KAlCoBBa0-glass** samples.

± 0.001 g cm^{-3}, with further addition of barium content. This increase is due to the differences in the molecular weight (K_2 = 94.20 g mol^{-1} and BaO = 153.3 g mol^{-1}). In addition to the change in density of oxides, where the density of (BaO = 5.72 g cm^{-3}) while the density of (K_2O = 2.35 g cm^{-3}). Furthermore, the theoretical density was calculated of the studied composition. The theoretical density is presented in Fig. 2 (a). It behaved the same trend of increasing of the experimental density from 2.721 g cm^{-3} reaching 3.395 g cm^{-3} (i.e., increased to 25 %), with further addition of barium content. It is worth noting that no information was extracted about the glass structure from theoretical density. However, the theoretical density was calculated just to compare its values to the experimental ones. It is observed that the theoretical density has values higher than that of the experimental density, as shown in Fig. 2 (a). Such difference between them originates from the amorphous nature of our glasses [25]. This also confirms the right preparation of our samples in non-crystalline entity. Same increased density was observed when barium oxide loaded in different borate glass hosts [26,27]. However, the increasing rate for this glass host reaches 25 %, this obtained ratio is larger than that obtained in the previous works.

Additionally, the molar volume (V_m) is computed from the following relation [4,5]:

$$V_m = \frac{molecular\ weight}{measured\ density} \tag{1}$$

The calculated molar volume values were noticed to mitigate from 37.492 cm^{3}mol^{-1} reaching 32.580 cm^{3}mol^{-1} (i.e., down to ~ 15 %), with an experimental error about ± 0.001 cm^{3}mol^{-1}, with the increase in barium oxide, as depicted in Fig. 2 (b). The decrement in V_m is ascribed to the difference in V_m of the oxides (K_2O = 40.08 cm^{3}mol^{-1} and BaO = 26.66 cm^{3}mol^{-1}). Additional confirmative factors were calculated to support the molar volume behavior. One of these factors is the average boron-boron separation (d_{B-B}). The d_{B-B} was calculated from the following relation [4,5]:

$$d_{B-B} = \left[\frac{V_m}{2N_A(1-X_B)}\right]^{1/3} \tag{2}$$

where N_A is Avogadro's number. X_B is the boron oxide concentration. The obtained values of average boron-boron separation were detected to mitigate from 0.339 nm deteriorating to 0.300 nm (i.e., down to ~ 1 Å). This mitigation is a subtle indicator for the network constriction [7].

Other additional parameter of physical properties of the studied glass is the Ba^{2+} ion concentration (N_{Ba}) of the doping samples. The Ba^{2+} ion concentration (N_{Ba}) is determined from the next relation [4,5]:

$$N_{Ba} = \frac{N_A \times \text{conc. of BaO}}{V_m} \tag{3}$$

The attained values of Ba^{2+} ion concentrations were found to normally enhances from 8.40×10^{20} ionscm^{-3} up to 37.00×10^{20} ionscm^{-3} with adding the barium oxide contents. This increased behavior is acceptable trend due to increasing barium oxide contents. Also, the calculation of inter-atomic distance (R_i) of doping samples contributes to evaluate the impact of alkalinity modification. The inter-atomic distance (R_i) is estimated from the next relation [4,5]:

$$R_i = \left[\frac{1}{N_{Ba}}\right]^{1/3} \tag{4}$$

where N_{Ba} is the barium ions concentrations. The resulting values of inter-atomic distance were found to mitigate from 1.059 nm up to 0.647 nm (i.e., decreased to ~ 4.12 Å) with increasing of the barium oxide contents. This decrease is back to that: the insertion of Ba^{2+} cations mitigates the interatomic distances with surroundings based on that the ionic radius of barium cation (268 Pm) is lower than that of potassium ion (280 Pm) [28]. Hence, the increased density confirmed the densification of network, while the mitigation in network volume was confirmed by the calculation of V_m, average boron-boron separations and interatomic distances [29,30]. It is observed that the alkalinity changes from alkali (potassium) to alkaline (barium) has a clear impact on the network modification, briefly, the additions of barium oxides lead to more densification of network and more contraction of its volume. All structural parameters were recorded in Table 1.

3.2. Vibrational spectroscopy

FT-IR spectroscopy is the main tool for investigating the structural changes in amorphous solids and identifying of ligand field inside the

Table 1
Experimental and theoretical density (ρ), molar volume (V_m), the average boron-boron separation ($d_{B\text{-}B}$), interatomic distance (R_i), and Ba^{2+} ions concentration (N_{Ba}) of all glass samples.

Sample (mol. %)	ρ_{Exp} (g/cm^3) ±0.001	$\rho_{Theort.}$ (g/cm^3)	V_m (cm^3/mol) ±0.001	d_{B-B} (nm) ±0.001	R_i (nm) ±0.001	$N_{Ba^{2+}}$ (× 10^{20}/cm^3) ±0.001 × 10^{20}
KAlCoBBa-0	2.120	2.721	37.492	0.339	0.000	0.00
KAlCoBBa-5	2.302	2.890	35.801	0.327	1.059	8.40
KAlCoBBa-10	2.454	3.058	34.797	0.318	0.833	17.30
KAlCoBBa-15	2.643	3.227	32.998	0.307	0.715	27.40
KAlCoBBa-20	2.802	3.395	32.580	0.300	0.647	37.00

glass network. Moreover, it provides a clarification of the interplay between alkali/alkaline cations and borate glassy networks. The measured infrared spectra of [BaO-K_2-B_2O_3-CoO-Al_2O_3] glass systems are presented in Fig. 3 (a). It is observed that the infra-red spectra are broad, therefore a Gaussian deconvolution processes are necessary to decompose the overlapping between infrared bands. A representative figure for the deconvoluted infrared peaks is presented in Fig. 2 (b). The attained peaks from deconvolution processes are assigned and tabulated in Table 2.

weak absorption bands at ~454 cm^{-1} (highlighted with yellow color) was observed in the beginning of infrared spectra, which may be due to the alkali content [31]. The absorbance of this band was observed to exponentially decrease from 0.015 reaching 0.004 with the additions of BaO contents, as exhibited in Fig. 4. Therefore, it is decisively expected that this band may be related to specific K–O bonds vibrations. Unusually, the alkali-oxygen bonds appear as extended above 400 cm^{-1} tails, however, the vibrational band of these bonds has a clear infrared band, in addition its variation is touchable and well-explained. The

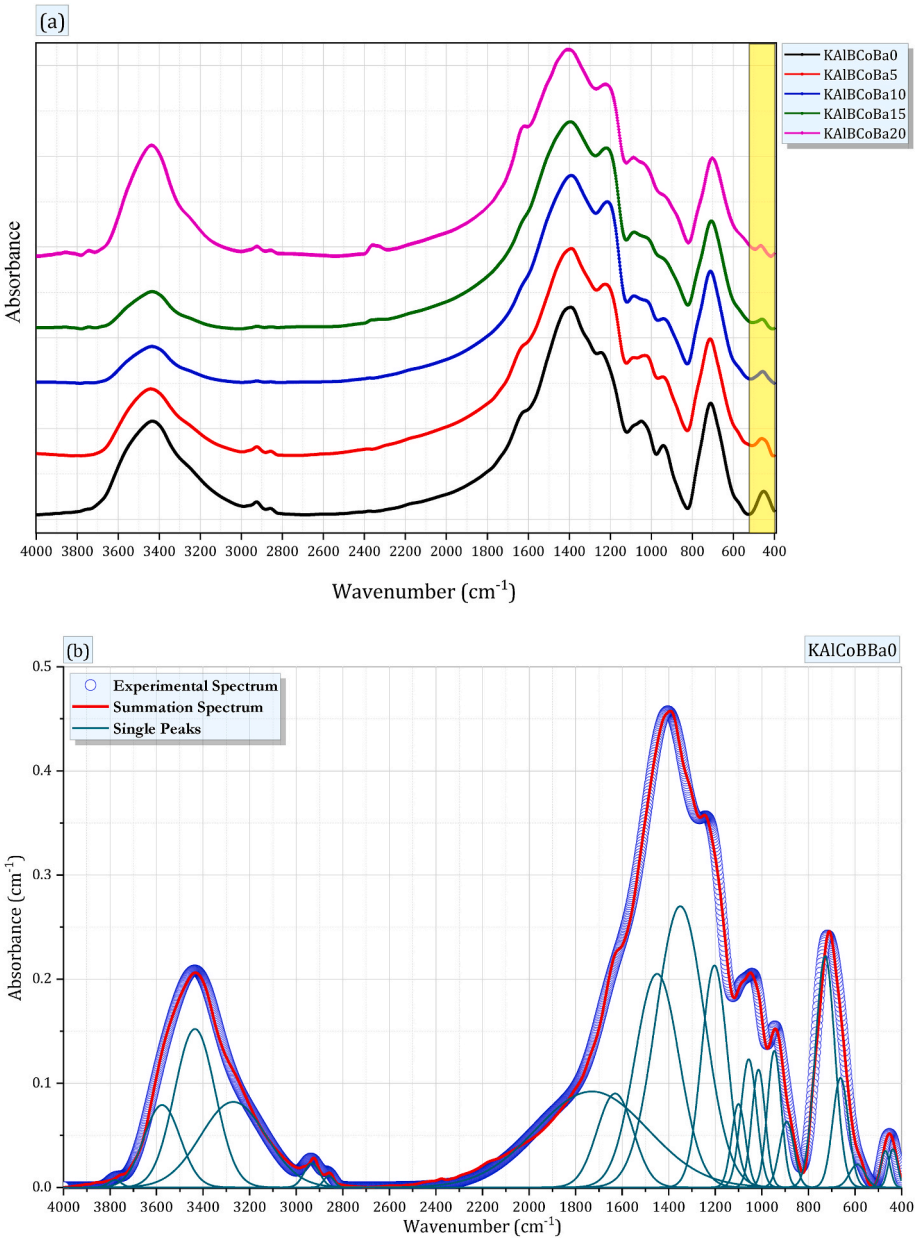

Fig. 3. (A)The measured infrared spectra for the studied glass system and (b) A representative figure for the deconvolution process for the **KAlBCoBa0-glass** sample.

Table 2
FTIR peak positions together with brief assignments of all glass samples.

Refs.	Wavenumber (cm^{-1})					Assignments
	0	5	10	15	20	
[30]	453	454.5	454.5	454.5	454.5	Alkali ions vibrations (K^+)
[7,9,12]	590	590	588	592	575	B–O–B bending vibrations as well as borate ring angle's deformations/and $Co^{3+}-O$ bonds
[31]	662	668	670	670	655	B–O symmetric stretching vibrations of BO_3 units
[4]	728	733	731	725	720	Stretching vibrations of Al–O bonds in AlO_6 network units
[32]	893	875	880	880	888	Al–O bonds in AlO_4 structural units
[7,34,35]	946	940	940	950	947	B–O stretching vibrations of non-bridging oxygen's of tetrahedral units, $(NBOs)_{BO_4}$
[7,34,35]	1014	1014	1012	1013	1011	B–O stretching vibrations and rocking motion of tetrahedral BO_4 units.
[7,34,35]	1056	1055	1062	1057	1059	
[32,33]	1100	1095	1090	1090	1090	Al–O bonds in AlO_4 structural units
[34–36]	1203	1197	1202	1199	1197	B–O symmetric stretching vibrations of non-bridging oxygens of trigonal units, $(NBOs)_{BO_3}$.
[34–36]	1350	1346	1347	1338	1342	B–O asymmetric
[34–36]	1450	1459	1460	1469	1462	stretching vibrations of BO_3 units
[37]	1630	1635	1618	1636	1632	OH- in B–O
	1730	1735	1735	1735	1735	
[37–39]	2860	2860	2860	2860	2860	OH
	2933	2933	2933	2933	2933	
	3270	3270	3280	3295	3300	
	3435	3435	3430	3439	3435	
	3576	3550	3550	3557	3555	
	3780	3780	3780	3770	3780	

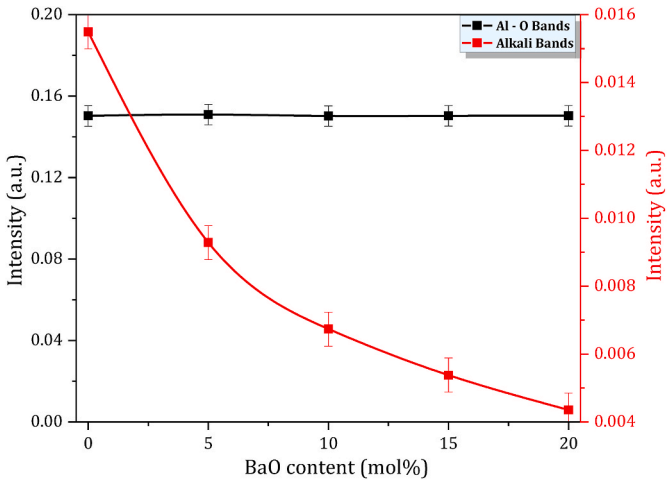

Fig. 4. The intensity of deconvoluted infrared bands for all aluminum and alkali bands of the prepared system.

absorption bands at ~587 cm^{-1} are assigned to B–O–B bending vibrations and borate rings angle deformations [7], and it may be due to specific vibrations of Co^{3+}-O group indicating a possible presence of cobalt cations in trivalent states, which occupy octahedral sites [9,12]. The located band at ~660 cm^{-1} is associated with the symmetric bonds of bending vibrations of B–O–B of bridging oxygens in BO_3 units [32–34].

The additions of aluminum oxide in the glassy network leads to modify the network to new structure. These aluminum ions are associating with the boron and oxygen in the networks to form new bonds, producing new bands in the infrared spectra. One of important tasks of deconvolution process is to decompose these overlapping bands. The resulting bands in the infrared window were observed at ~727, 883 and 1095 cm^{-1}. The first band was observed to pin at ~727 cm^{-1} and is ascribed to stretching vibrations of Al–O bonds in AlO_6 network units [4]. The centered band at ~893 cm^{-1} is related to the vibrations of Al–O bonds in AlO_4 structural units [35]. The enveloped band at ~1100 cm^{-1} is created by the vibrations of Al–O bonds in AlO_4 structural units, which work as glass formers [35,36]. We detected that the intensity of Al–O bands is mostly unchanged with increasing barium oxide content as exhibited in Fig. 4. This means that the additions of barium oxide have inane effect to modify the structural units of aluminum oxide in the network.

Back again to borate network, the spectral absorption region from ~820 cm^{-1} to 1150 cm^{-1} is probably due to the B–O stretching vibrations of BO_4 structural units [7,37,38]. While the strong infrared absorption bands that appeared from ~1150 to 1700 cm^{-1} are created by the stretching vibration belongs to O_3 structural units. Specifically, B–O symmetric stretching vibrations belongs to nonbridging oxygen of trigonal units, $(NBOs)_{BO_3}$ was pinned at ~1200 cm^{-1} [39–41]. The existence of a band around ~1730 cm^{-1}, which overlaps with triangles BO_3 band, is due to the –OH bending vibrations [42]. As well as the band at ~2900–3800 cm^{-1} belongs to the water molecules, hydrogen bonding and B–OH in the glasses [43]. Finally, the band at ~3570 cm^{-1} is attributed to free OH stretching vibrations [44]. Moreover, the absorbance of OH band were detected to decrease with increasing BaO contents up to 10 mol % then starts to increase again, as shown in Fig. 3. This behavior suggests that the sample containing an equal content of mixed alkali (i.e., 10 mol% of BaO: 10 mol% of K_2O glass sample) absorbs less moisture. From the Gaussian deconvolution process of the infrared absorption bands, it is observed that the addition of barium content has soft impact on the structural units of network. For example, the intensity of alkali bands was observed to diminish from 1.6 % to 0.4 %, confirming that the observed infrared band, which pinned at ~454 cm^{-1}, related to the potassium oxide. The ratio of spectral area of aluminum bonds were found to not change and still constant at 15.04 %, while the N_4 and *NBO* that related to borate network were found to change slightly about the values at 12.31 % and 19.46 %, respectively. However, the content of barium was added by wide concentrations, the changes in the glass network were barely observed. Overall, the alkalinity modifications (i.e., change the alkaline oxide instead of alkali oxide) in such glass systems have soft impact on their network structural variations.

3.3. Optical properties

3.3.1. Ligand field parameters

For many decades, ligand field theorem was employed to study the structural modifications in the material based on the involved transition metal ion (here, cobalt) in the glass host. Studying the changes of the ligand field parameters leads to best understanding of the structural-optical relationships from their optical absorbance as shown in Fig. 5. These parameters depend on the structure of host glasses (specifically, on the surround ligand field of Co^{2+} ions), therefore small changes related to the composition such as the alkalinity modifications leads to a

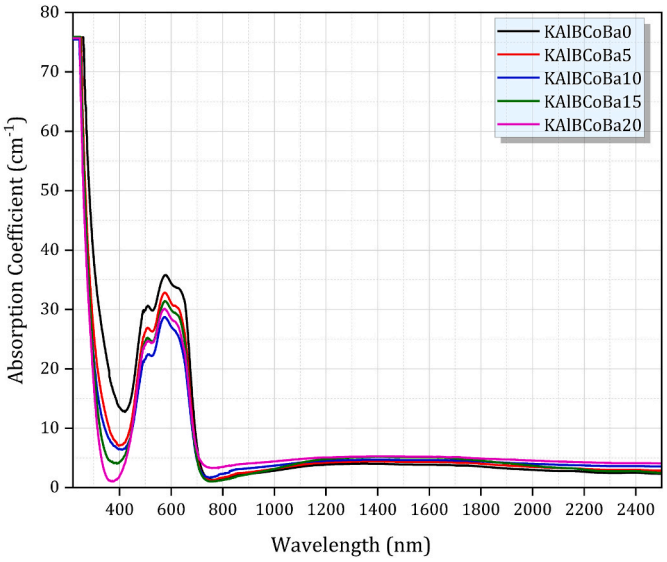

Fig. 5. The optical absorption coefficient of **KAlCoBBa-glass** samples measured at room temperature.

clear impact on the structural-optical features. These parameters are such as ligand field splitting (*10Dq*), Racah parameters (*B* and *C*), and nephelauxetic coefficient, and they shall be discussed in detail in the following paragraphs.

The Co^{2+} ions in glasses give a palette of colors from blue to pink. It is well-known the blue color is brought from Co^{2+} ions in tetrahedral positions, while the pink color is brought from Co^{2+} ions in octahedral positions. The site symmetry of Co^{2+} ions is controlled by tuning the ligand field around cobalt ions, for example, the alkalinity modifications is one of these controllers. For Co^{2+} ions in tetrahedral sites, two important optical transitions are exploited in ligand field calculations, the first transition is located at ~ 574 nm and is denoted as (ν_3), while the second one is located at ~ 1413 nm and is termed as (ν_2). These two bands are explicitly shown in Fig. 6. The *10Dq* (i.e., splitting) is a measure of the splitting energy of (d^7) orbitals of Co^{2+} ions in tetrahedral symmetry. While the Racah Parameter (*B* and *C*) are a measure of the repulsive force due to the interplay between the electrons of d-orbitals in Co^{2+} ions in tetrahedral symmetry. Their ligand field equations are given by Refs. [11–15]:

$$10\,Dq = \frac{1}{3}(\nu_2 + \nu_3) - 5B \tag{15}$$

$$B = \frac{1}{510}\left[7(\nu_2+\nu_3) \pm \left\{49(\nu_2+\nu_3)^2 + 680(\nu_2-\nu_3)^2\right\}^{\frac{1}{2}}\right] \tag{16}$$

$$C = 4.63\,B \tag{17}$$

where ν_2 and ν_3 are previously well-defined. The values of *10 Dq* (*B* and *C*) were found to mitigate (augment) with further addition of barium content. Fig. 7 shows the *10 Dq* against *B*, while *C* was recorded in Table 3. Such decrement (increment) in 10 *Dq* (*B* and *C*) is related to the alkalinity modifications. It is observed that the addition of alkaline content governed the interaction strength between Co ions and their anions. This is in its turns mitigated the interaction strength between *d*-orbitals of Co^{2+} ions and the ions of surrounding field [37]. The insertion of Ba^{2+} ions may decrease the network defects, which contain loosely bound electrons, consequently decreasing the electrons' ability to transfer across the band gap. This result is in a best agreement with the increase in E_{opt} and the decrease in E_U, as discussed before.

To push further, studying the increase in Racah parameters (*B* and *C*), with the insertion of Ba^{2+} ions content, is related to a strong field resulting from the repulsive interaction between the electrons in *d*-orbitals of Co^{2+} ions. Here, the effect of alkaline is clear. Due to the high field strength and lower ionic radius of barium ions, the interaction between Co ions and their surrounding anions was quenched, leading to minimize the splitting of *d*-orbitals in Co^{2+} ions. Additionally, this causes the d-orbitals to shrink, reducing the distances between d-electrons. As a result, according to Coulomb's law, the repulsive force between d-electrons increases. Furthermore, this d-orbitals shrinkage with high interaction between d-electrons of Co^{2+} ions result in a high tendency toward the ionicity of bond nature between Co^{2+} ions and their ligands. Same calculations of ligand field parameters 10 *Dq* and (*B* and *C*) of cobalt ions in alkali borate glass were obtained in literature [9,12,13,45]. However, the good ionic bonding nature were obtained for these glasses, this distinctive feature is required in designing of optoelectronic devices.

Furthermore, there are some valuable and ligand field related parameters, for example, the nephelauxetic ratios (β) is the ratios between *B* for Co cations inside glasses and its value for Co free cation [13] $\beta = B/B_o$, where B_o of cobalt free ion is 971 cm^{-1}. The obtained values of nephelauxetic ratio were reported in Table 3. The increase in these

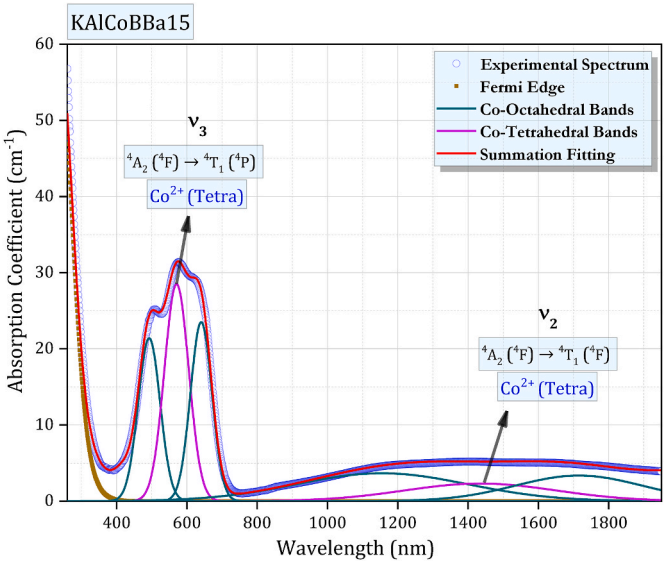

Fig. 6. Gaussian deconvoluted process of optical absorption coefficient spectrum of for **KAlCoBBa15-glass** sample as an example.

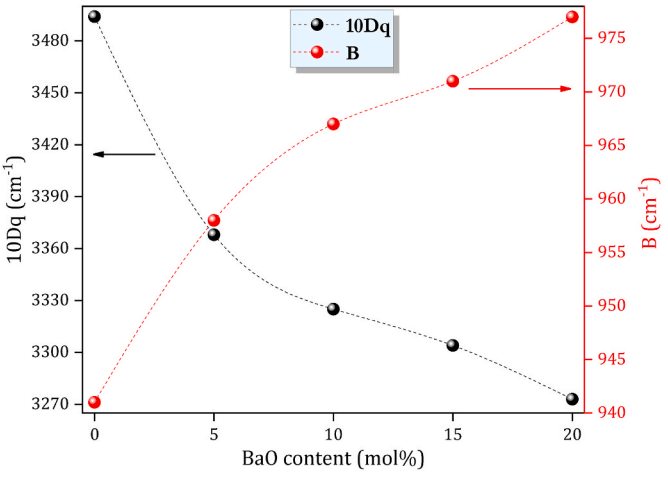

Fig. 7. Variation's ligand field splitting (10Dq) and Racah parameter (*B*) versus BaO content for **KAlCoBBa15-glass** samples.

Table 3
Band positions (λ ± 1 nm) and energy (E ± 5 cm^{-1}) values of electronic transitions (ν_2 and ν_3) of Co^{2+} ions, Racah parameter (C), nephelauxetic ratio (β), nephelauxetic parameter (β_1), covalency reduction factor (N^2), and Slater-Condon parameters (F_2 and F_4) for all glass samples.

Sample Code - mol%	$^4A_2(F) \rightarrow {}^4T_1(P)$ (ν_3)		$^4A_2(F) \rightarrow {}^4T_{1g}(F)$ (ν_2)		C (cm^{-1})	β	β_1	N^2	F_2	F_4
	(λ) nm	(*E*) cm^{-1}	(λ) nm	(*E*) cm^{-1}						
KAlCoBBa-0	582	17182	1350	7407	4355	0.969	1.370	0.98	1563	124
KAlCoBBa-5	576	17361	1405	7117	4437	0.987	1.395	0.99	1592	126
KAlCoBBa-10	572.8	17458	1425	7018	4476	0.996	1.408	0.99	1606	128
KAlCoBBa-15	571	17513	1435	6969	4497	1.000	1.414	1.00	1614	128
KAlCoBBa-20	569	17574	1450	6897	4523	1.006	1.423	1.00	1623	129

values implies that there is an increasing in ionicity of bond nature between Co^{2+} ions and their surrounding field [46]. For more provision confirmation concerning the formed bond nature, nephelauxetic parameter (β_1) should be calculated from the following relation [38]:

$$\beta_1 = \sqrt{\left(\frac{B}{B_o}\right)^2 + \left(\frac{C}{C_o}\right)^2} \quad (18)$$

Brik and Srivastava [47] were proposed this new nephelauxetic parameter (β_1) to treat the defect in the old nephelauxetic ratio ($\beta = B/B_o$). The nephelauxetic ratio ($\beta = B/B_o$) describes the electronic cloud in *d*-orbitals only based on Racah *B* parameter. However, the proposed relation by Brik and Srivastava included both Racah (*B* and *C*) parameters. The obtaining values of the β_1 parameter are reported in Table 3. It is monitored that there is an enhancement in β_1 values, confirming the ionic bond nature. Ba^{2+} ions have ionic radius greater than that for K^+ ions, therefore the increase in interionic separations leads to an enhancement in β_1 values, improving the ionicity nature between Co^{2+} ions and their ligands.

Furthermore, information about the bond nature is the covalency reduction factor, N^2, that traces the covalency of bonding nature in materials. The covalency reduction factor can be extracted from the following relationship [7]:

$$N^2 = \frac{1}{2}\left(\sqrt{\frac{B}{B_o}} + \sqrt{\frac{C}{C_o}}\right) \quad (19)$$

when the covalency reduction factor increases, the covalency in bonding nature shrinks and vice-versa. The attained values of N^2 are recorded in Table 3. The increase in covalency reduction factor relates to the covalency reduction effects with the progressive addition of barium oxide (i.e., electron-electron repulsion increases).

Finally, the Slater-Condon [37] were proposed a linear representation that combines the ligand field parameters to describe the energy of *d*-orbitals.

$$F_2 = B + \frac{C}{7} \quad (20)$$

$$F_4 = \frac{C}{35} \quad (21)$$

The attained values of F_2 and F_4 are registered in Table 3. Slater-Condon parameters were found to increase, exhibiting an opposite propensity to *10Dq*. This increase in Slater -Condon parameters is related to ionicity enhancement, which has created from the alkalinity modifications.

4. Conclusion

In this work, the effect of BaO on structure and optical properties of cobalt alumino-borate was studied. Detailed structural and optical properties were evaluated in terms of increasing the barium oxide content. The density increased from 2.120 g cm^{-3} up to 2.802 g cm^{-3}. The related parameters such as molar volume, average boron-boron separations, and inter-atomic distances revealed densification with more contraction of the alumino-borate network. Deconvolution of FT-IR spectra confirmed the presence of AlO_4, AlO_6, BO_3, and BO_4 structural units, with soft conversion between these structural units. Interestingly, the 10 K_2O:10 BaO glass sample exhibits less absorbance of moisture since the intensity of OH- band decreased. The further additions of BaO caused an increase in Racah parameters and a decrease in ligand field strength. moreover, the nephelauxetic effect exhibits an increase in the ionicity of the bond nature with more BaO additions.

CRediT authorship contribution statement

Hesham Y. Amin: Writing – review & editing, Writing – original draft, Resources, Methodology, Conceptualization. **A. Samir:** Writing – original draft, Methodology. **Moukhtar A. Hassan:** Writing – original draft, Methodology, Formal analysis, Conceptualization. **F. Ahmad:** Writing – original draft, Investigation. **Aly Saeed:** Resources. **M.S. Sadeq:** Writing – review & editing, Writing – original draft, Methodology, Investigation, Conceptualization.

Declaration of competing interest

The authors declare that they have no known competing financial interests or personal relationships that could have appeared to influence the work reported in this paper.

Data availability

Data will be made available on request.

References

[1] L. Singh, V. Thakur, R. Punia, R.S. Kundu, A. Singh, Structural and optical properties of barium titanate modified bismuth borate glasses, Solid State Sci. 37 (2014) 64–71, https://doi.org/10.1016/j.solidstatesciences.2014.08.010.

[2] E.A. Elkelany, M.A. Hassan, A. Samir, A.M. Abdel-Ghany, H.H. El-Bahnasawy, M. Farouk, Optical and Mössbauer spectroscopy of lithium tetraborate glass doped with iron oxide, Opt. Mater. 112 (2021) 110744, https://doi.org/10.1016/j.optmat.2020.110744.

[3] M.A. Hassan, Effect of halides addition on the ligand field of chromium in alkali borate glasses, J. Alloys Compd. 574 (2013) 391–397, https://doi.org/10.1016/j.jallcom.2013.05.177.

[4] H.Y. Morshidy, M.S. Sadeq, A.R. Mohamed, M.M. EL-Okr, The role of CuCl2 in tuning the physical, structural and optical properties of some Al2O3–B2O3 glasses, J. Non-Cryst. Solids 528 (2020) 28–29, https://doi.org/10.1016/j.jnoncrysol.2019.119749.

[5] H.Y. Morshidy, M.S. Sadeq, In Fl Uence of Cobalt Ions on the Structure , Phonon Emission , Phonon Absorption and Ligand Fi Eld of Some Sodium Borate Glasses, 2019, p. 525.

[6] S.C. Colak, E. Aral, Optical and thermal properties of P2O5-Na 2O-CaO-Al2O3:CoO glasses doped with transition metals, J. Alloys Compd. 509 (2011) 4935–4939, https://doi.org/10.1016/j.jallcom.2011.01.172.

[7] H.Y. Morshidy, Z.M. Abd El-Fattah, A.A. Abul-Magd, M.A. Hassan, A.R. Mohamed, Reevaluation of C r 6 + optical transitions through G d 2 O 3 doping of chromium-borate glasses, Opt. Mater. 113 (2021) 110881, https://doi.org/10.1016/j.optmat.2021.110881.

[8] M.O.J.Y. Hunault, L. Galoisy, G. Lelong, M. Newville, G. Calas, Effect of cation field strength on Co2+ speciation in alkali-borate glasses, J. Non-Cryst. Solids 451 (2016) 101–110, https://doi.org/10.1016/j.jnoncrysol.2016.06.025.

[9] P. Naresh, G. Naga Raju, C. Srinivasa Rao, S.V.G.V.A. Prasad, V. Ravi Kumar, N. Veeraiah, Influence of ligand coordination of cobalt ions on structural properties of ZnO-ZnF 2-B 2O 3 glass system by means of spectroscopic studies, Phys. B

Condens. Matter 407 (2012) 712–718, https://doi.org/10.1016/j.physb.2011.12.007.
[10] G. Lakshminarayana, S. Buddhudu, Spectral analysis of Mn2+, Co2+ and Ni2+: B2O3-ZnO-PbO glasses, Spectrochim. Acta Part A Mol. Biomol. Spectrosc. 63 (2006) 295–304, https://doi.org/10.1016/j.saa.2005.05.013.
[11] F. Ahmad, E. Hassan Aly, M. Atef, M.M. Elokr, Study the influence of zinc oxide addition on cobalt doped alkaline earth borate glasses, J. Alloys Compd. 593 (2014) 250–255, https://doi.org/10.1016/j.jallcom.2014.01.067.
[12] Z.M. Abd El-Fattah, F. Ahmad, M.A. Hassan, Tuning the structural and optical properties in cobalt oxide-doped borosilicate glasses, J. Alloys Compd. 728 (2017) 773–779, https://doi.org/10.1016/j.jallcom.2017.09.059.
[13] A.A. Abul-Magd, A.S. Abu-Khadra, A.M. Abdel-Ghany, Influence of La2O3 on the structural, mechanical and optical features of cobalt doped heavy metal borate glasses, Ceram. Int. 47 (2021) 19886–19894, https://doi.org/10.1016/j.ceramint.2021.03.326.
[14] A.A. El-daly, M.A. Abdo, H.A. Bakr, M.S. Sadeq, Impact of cobalt ions on the phonon energy and ligand field parameters of some borate glasses, J. Non-Cryst. Solids 555 (2021) 120535, https://doi.org/10.1016/j.jnoncrysol.2020.120535.
[15] M.M. Morsi, S. El-Konsol, M.I. El-Shahawy, Optical spectra of borate glasses containing Ti and Co in relation to their structure, J. Non-Cryst. Solids 83 (1986) 241–250, https://doi.org/10.1016/0022-3093(86)90239-5.
[16] P. Pascuta, S. Rada, G. Borodi, M. Bosca, L. Pop, E. Culea, Influence of europium ions on structure and crystallization properties of bismuth-alumino-borate glasses and glass ceramics, J. Mol. Struct. 924–926 (2009) 214–220, https://doi.org/10.1016/j.molstruc.2009.01.003.
[17] V.R.L. Murty, M. Venkateswarlu, K. Swapna, S. Mahamuda, P. Rekha Rani, A. S. Rao, Optical and spectroscopic studies of Dy3+ ions doped Alumino tungsten borate glasses for w-LEDs applications, Polyhedron 227 (2022) 116137, https://doi.org/10.1016/j.poly.2022.116137.
[18] E. Barney, N. Laorodphan, F. Mohd-Noor, D. Holland, T. Kemp, D. Iuga, R. Dupree, Toward a structural model for the aluminum tellurite glass system, J. Phys. Chem. C 124 (2020) 20516–20529, https://doi.org/10.1021/acs.jpcc.0c04342.
[19] M.S. Sadeq, H.Y. Morshidy, Effect of samarium oxide on structural, optical and electrical properties of some alumino-borate glasses with constant copper chloride, J. Rare Earths 38 (2020) 770–775, https://doi.org/10.1016/j.jre.2019.11.003.
[20] H. Doweidar, Y.M. Moustafa, S. Abd El-Maksoud, H. Silim, Properties of Na2O-Al2O3-B2O3 glasses, Mater. Sci. Eng. 301 (2001) 207–212, https://doi.org/10.1016/S0921-5093(00)01786-X.
[21] S. Mohan, S. Kaur, P. Kaur, D.P. Singh, Spectroscopic investigations of Sm3+-doped lead alumino-borate glasses containing zinc, lithium and barium oxides, J. Alloys Compd. 763 (2018) 486–495, https://doi.org/10.1016/j.jallcom.2018.05.319.
[22] J.D.M. Dias, G.H.A. Melo, T.A. Lodi, J.O. Carvalho, P.F. Façanha Filho, M. J. Barboza, A. Steimacher, F. Pedrochi, Thermal and structural properties of Nd2O3-doped calcium boroaluminate glasses, J. Rare Earths 34 (2016) 521–528, https://doi.org/10.1016/S1002-0721(16)60057-1.
[23] P. Kaur, S. Kaur, G.P. Singh, D.P. Singh, Cerium and samarium codoped lithium aluminoborate glasses for white light emitting devices, J. Alloys Compd. 588 (2014) 394–398, https://doi.org/10.1016/j.jallcom.2013.10.181.
[24] M.S. Sadeq, M.A. Abdo, Effect of iron oxide on the structural and optical properties of alumino-borate glasses, Ceram. Int. 47 (2021) 2043–2049, https://doi.org/10.1016/j.ceramint.2020.09.036.
[25] A.K. Varshneya, Fundamentals of Inorganic Glasses, Academic Press, Inc., 1994.
[26] A.M. Babeer, M.I. Sayyed, H.Y. Morshidy, A.E. Mahmoud, M.A. Abdo, M.S. Sadeq, High transparency of PbO–BaO–Fe2O3–SrO–B2O3 glasses with improved radiation shielding properties, Opt. Mater. 145 (2023) 114387, https://doi.org/10.1016/j.optmat.2023.114387.
[27] M.I. Sayyed, H.Y. Morshidy, K.S. Shaaban, A.F.A. El-Rehim, A.M. Ali, M.S. Sadeq, Impacts of BaO additions on structure, linear/nonlinear optical properties and radiation shielding competence of BaO–NiO–ZnO–B2O3 glasses, Opt. Mater. 144 (2023) 114300, https://doi.org/10.1016/j.optmat.2023.114300.
[28] Y.B. Saddeek, K.A. Aly, K.S. Shaaban, A.M. Ali, M.A. Sayed, Elastic, optical and structural features of wide range of CdO- Na2B4O7 glasses, Mater. Res. Express 5 (2018) 65204, https://doi.org/10.1088/2053-1591/aac93f.
[29] A.I. Ismail, A. Samir, F. Ahmad, L.I. Soliman, A. Abdelghany, The effect of radiation on the structure and ligand field of borate glasses containing Cr ions, Opt. Quant. Electron. 53 (2021) 1–15, https://doi.org/10.1007/s11082-021-02740-2.
[30] M. Farouk, Effect of Co2+ ions on the ligand field , optical , and structural properties of ZnLiB glasses, Optik 140 (2017) 186–196.
[31] M.A. Hassan, F.M. Ebrahim, M.G. Moustafa, Z.M. Abd El-Fattah, M.M. El-Okr, Unraveling the hidden Urbach edge and Cr 6+ optical transitions in borate glasses, J. Non-Cryst. Solids 515 (2019) 157–164, https://doi.org/10.1016/j.jnoncrysol.2019.02.026.
[32] E.I. Kamitsos, A.P. Patsis, M.A. Karakassides, G.D. Chryssikos, Infrared reflectance spectra of lithium borate glasses, J. Non-Cryst. Solids 126 (1990) 52–67, https://doi.org/10.1016/0022-3093(90)91023-K.
[33] M. Ezzeldien, H.Y. Morshidy, A.M. Al-boajan, A.M. Al Souwaileh, Z.A. Alrowaili, M.S. Sadeq, Environmental impacts of La2O3 on the optical and ligand field parameters of Ni ions inside Na2O-B2O3 glass, J. Alloys Compd. 961 (2023) 170891, https://doi.org/10.1016/j.jallcom.2023.170891.
[34] M.S. Sadeq, M.I. Sayyed, A.E. Mahmoud, M.A. Abdo, H.E. Ali, H.Y. Morshidy, Composition dependence of transparency, optical, ligand field and radiation shielding properties in CdO–Fe2O3–Na2O–B2O3 glasses, Ceram. Int. 49 (2023) 28175–28188, https://doi.org/10.1016/j.ceramint.2023.06.071.
[35] F. Ahmad, E. Nabhan, Spectroscopic and mechanical studies of lithium aluminoborate glasses doped with chromium ions, Opt. Quant. Electron. 51 (2019) 1–14, https://doi.org/10.1007/s11082-019-1973-y.
[36] M. Walas, A. Pastwa, T. Lewandowski, A. Synak, I. Gryczyński, W. Sadowski, B. Kościelska, Luminescent properties of Ln3+ doped tellurite glasses containing AlF3, Opt. Mater. 59 (2016) 70–75, https://doi.org/10.1016/j.optmat.2016.01.040.
[37] H.Y. Morshidy, A.R. Mohamed, A.A. Abul-magd, M.A. Hassan, Role of high energy Cr 6 + optical transition induced by rare earth ion (La 3 +) in compositional-dependent borate glass, Mater. Chem. Phys. 289 (2022) 126503, https://doi.org/10.1016/j.matchemphys.2022.126503.
[38] H.Y. Morshidy, A.R. Mohamed, A.A. Abul-magd, M.A. Hassan, Ascendancy of Cr 3 + on Cr 6 + valence state and its effect on borate glass environment through CdO doping, Mater. Chem. Phys. 285 (2022) 126128, https://doi.org/10.1016/j.matchemphys.2022.126128.
[39] A.A. Abul-Magd, H.Y. Morshidy, A.M. Abdel-Ghany, The role of NiO on the structural and optical properties of sodium zinc borate glasses, Opt. Mater. 109 (2020), https://doi.org/10.1016/j.optmat.2020.110301.
[40] H.Y. Morshidy, E.A. Elkelany, K.T. Abul-Nasr, A. Samir, H.H. El-Bahnasawy, M. A. Hassan, Fe57 Mössbauer, optical and structural properties with ligand field effects of borosilicate glass doped with iron oxide, Mater, Today Commun. 37 (2023) 106917, https://doi.org/10.1016/j.mtcomm.2023.106917.
[41] M.M. EL-Hady, H.Y. Morshidy, M.A. Hassan, Judd-Ofelt analysis, optical and structural features of borate glass doped with erbium oxide, J. Lumin. 263 (2023) 119972, https://doi.org/10.1016/j.jlumin.2023.119972.
[42] F. Ahmad, Study the effect of alkali/alkaline earth addition on the environment of borochromate glasses by means of spectroscopic analysis, J. Alloys Compd. 586 (2014) 605–610, https://doi.org/10.1016/j.jallcom.2013.10.105.
[43] D. Singh, K.S. Thind, G.S. Mudahar, B.S. Bajwa, Optical absorption and infrared spectroscopic analysis of γ-irradiated ZnO-BaO-B2O3 glasses, Nucl. Instrum. Methods Phys. Res. Sect. B Beam Interact. Mater. Atoms 268 (2010) 3340–3343, https://doi.org/10.1016/j.nimb.2010.07.007.
[44] F.A. Moustafa, A.M. Fayad, F.M. Ezz-Eldin, I. El-Kashif, Effect of gamma radiation on ultraviolet, visible and infrared studies of NiO, Cr2O3 and Fe2O3-doped alkali borate glasses, J. Non-Cryst. Solids 376 (2013) 18–25, https://doi.org/10.1016/j.jnoncrysol.2013.04.052.
[45] M.G. Moustafa, H. Morshidy, A.R. Mohamed, M.M. El-Okr, A comprehensive identification of optical transitions of cobalt ions in lithium borosilicate glasses, J. Non-Cryst. Solids 517 (2019) 9–16, https://doi.org/10.1016/j.jnoncrysol.2019.04.037.
[46] C.G. Ma, Y. Wang, D.X. Liu, Z. Li, X.K. Hu, Y. Tian, M.G. Brik, A.M. Srivastava, Origin of the β1 parameter describing the nephelauxetic effect in transition metal ions with spin-forbidden emissions, J. Lumin. 197 (2018) 142–146, https://doi.org/10.1016/j.jlumin.2018.01.036.